Natural Resources Canada | Ressources naturelles Canada

GEOLOGICAL SURVEY OF CANADA
OPEN FILE 8903

Organic petrography and thermal maturity of the Paskapoo Formation in the Fox Creek area, west-central Alberta

O.H. Ardakani

2022

Canada

ISSN 2816-7155
ISBN 978-0-660-44272-3
Catalogue No. M183-2/8903E-PDF

GEOLOGICAL SURVEY OF CANADA
OPEN FILE 8903

Organic petrography and thermal maturity of the Paskapoo Formation in the Fox Creek area, west-central Alberta

O.H. Ardakani

2022

Permanent link: https://doi.org/10.4095/330296

This publication is available for free download through GEOSCAN (https://geoscan.nrcan.gc.ca/).

Recommended citation
Ardakani, O.H., 2022. Organic petrography and thermal maturity of the Paskapoo Formation in the Fox Creek area, west-central Alberta; Geological Survey of Canada, Open File 8903, 20 p. https://doi.org/10.4095/330296

Publications in this series have not been edited; they are released as submitted by the author.

Table of Contents

Abstract

The Paskapoo Formation, which ranges in age from middle to upper Paleocene, is the major shallow aquifer in Alberta. This study is part of a larger GSC-led study on the potential environmental impact of hydrocarbon development in the Fox Creek area (west-central Alberta) on shallow aquifers. Fox Creek is located near the northern limit of the Paskapoo Formation. In addition to the underlying organic-rich source rocks in the study area, including the Duvernay Formation that is currently exploited for hydrocarbon resources, the Paskapoo Formation contains organic-rich intervals and coal seams. In order to investigate any potential internal hydrocarbon sources within the Paskapoo Formation, ninety-seven (97) cutting samples from the formation obtained from eight shallow monitoring wells (50-90 m) in the study area were studied for total organic carbon (TOC) content, organic matter composition and thermal maturity of coal seams using programmed pyrolysis analysis and organic petrography.

The TOC content of all samples ranges from 0.2 to 8.8 wt. %, with a mean value of 0.95 ± 1.6 wt. % (n=97). The Tmax values of studied samples range from 347 to 463 °C, with a mean value of 434 ± 20 °C that suggest a range of thermal maturity from immature to peak oil window. The random reflectance (R_r) measurement and fluorescence microscopy on eighteen (18) selected samples with TOC content > ~1 wt. % shows a mean R_r value of 0.27% and 0.42% for the overlying till deposits and the underlying shallow depth sandstone, siltstone, shale and coal seams respectively, indicating a low rank coal ranging from lignite to sub-bituminous coal. Blue to green and yellow fluorescing liptinite macerals further confirmed the low maturity of studied samples. The low S2 yield of a large part of the samples (65%) resulted in unreliable Tmax values that overestimated the thermal maturity.

Although the organic matter in the studied intervals are immature, exsudatinite, as secondary liptinite maceral, was observed in samples from the lower parts of the studied monitoring wells. Exsudatinite generally derives from the transformation of sporinite, alginite, resinite and varieties of vitrinite, which is a resinous or asphalt like material. Considering the thickness and distribution of coal seams in the studied samples, it is unlikely the exsudatinite will be a major source for aquifer hydrocarbon contamination in the study area. Additional stratigraphic studies and molecular geochemical analysis could provide an estimate of the total volume of possible organic compounds contribution to the aquifer in the study area. Due to the presence of coal seams in the studied intervals of the Paskapoo Formation, it is important to investigate the possibility of biogenic methane formation in Paskapoo shallow aquifers.

Introduction

One of the major concerns of hydraulic fracturing is the leakage or migration of hydrocarbon and hydraulic fracturing fluids to shallow aquifers through natural fractures and/or induced fractures during hydraulic fracturing (Vidic et al., 2013; Flewelling and Sharma, 2014; Ryan et al., 2015; Digiulio and Jakson, 2016 among many others) or from activities at the surface (e.g., a spill). The Fox Creek area has been one of the most active hydrocarbon development domains in Canada over the last few decades, with production primarily from the Devonian Duvernay Formation. Directional drilling and hydraulic fracturing, fundamental technologies for economic production of these unconventional hydrocarbons, have been extensively used in this area.

The Environmental Geoscience and Groundwater Geoscience programs have developed a joint 5-year project (2019-2024) for the evaluation and understanding of potential environmental impacts of hydrocarbon development on shallow aquifers in the Fox Creek area in west-central Alberta. In the initial phase of the project, Lavoie et al. (2021) published an analysis of historical and new organic matter data, gas composition and isotopic ratios of deep hydrocarbon source rocks as part of this GSC-led project.

The previous study provided the fundamental data in order to evaluate the deep source(s) of dissolved hydrocarbons. In the event that dissolved hydrocarbons with a thermogenic signature were to be found in shallow groundwater of this region, this information would help determine their provenance. This study provides insights into total organic carbon (TOC) content, organic matter type, and its thermal maturity in the upper part of the Paskapoo Formation, the major shallow aquifer in Alberta (Grasby et al., 2008; Smerdon et al., 2019). The Paskapoo Formation comprises gray thick-bedded sandstone, siltstone, sandy mudstone, and coal seams (Fig. 1) that were deposited in a non-marine environment (Demchuk and Hills, 1991; Hamblin, 2004). These coal seams could be possible internal source of hydrocarbons in the aquifer, which would have a biogenic isotopic signature.

To investigate the TOC content, thermal maturity and hydrocarbon potential of the Paskapoo Formation coal seams, ninety-seven (97) cutting samples obtained from eight shallow monitoring wells (Table 1; Fig. 2) drilled in the Fox Creek area for the project were analysed using programmed pyrolysis. Organic petrography, fluorescence microscopy, and random reflectance measurements were also used to identify the major organic matter components of the studied intervals, as well as to confirm their thermal maturity.

Geological Setting

Paskapoo Formation

The Paskapoo Formation represents a vast eastward thinning wedge of non-marine sediments deposited from the rising of Cordillera into the Western Canada Sedimentary Basin (WCSB). It extends over more than 65,000 km^2 in western Alberta and ranges in thickness from zero to 800 m, and represents the youngest bedrock deposits in the WCSB (Grasby et al., 2008; Hamblin, 2004). The Paleozoic–Mesozoic units from the emerging mountains were the main source of sediments for the Paskapoo Formation (Garsby et al. 2008). The Paskapoo Formation strata range in age from middle to upper Paleocene (Fig. 1) (Demchuk and Hills, 1991). A mid-Paleocene basin wide, erosional unconformity forms the base of the Paskapoo Formation (Lerbekmo and Sweet 2000). The Paskapoo Formation comprises gray thick-bedded sandstone with buff weathering color and greenish siltstone, sandy mudstone and coal seams that were deposited in a non-marine environment (Hamblin, 2004).

In the central Alberta Plains, the Paskapoo Formation was divided into three members: (1) a lower Haynes Member, (2) an upper Lacombe Member and, (3) the Dalehurst Member, a laterally equivalent unit to the Lacombe Member (Demchuk and Hills, 1991) (Fig. 1). The Haynes and Lacombe members are recognizable in both outcrop and subsurface in the Red Deer-Lacombe area and can be correlated in the subsurface to the Alberta Foothills (Demchuk and Hills, 1991).

Haynes Member

The Haynes Member overlies erosional contact and is comprised of medium- to coarse-grained sandstone, minor conglomerate throughout as lag deposits overlying erosional contacts and subordinate siltstone, mudstone, shale and coal beds (Demchuk and Hills, 1991). The sandstone is light grey in fresh exposure and yellowish-brown in outcrop and predominantly massive with minor trough and planar cross-bedding, rare ripple lamination, rooting traces, and plant fragments. Paleontological studies of the Haynes Member including vertebrate and invertebrate paleontology (Allan and Sanderson, 1945; Fox, 1990) and palynology (Demchuk, 1990) confirm the Paleocene age for this member of the Paskapoo Formation (Demchuk and Hills, 1991).

Lacombe Member

The Lacombe Member is comprised of interbedded siltstone, mudstone, shale and coal with subordinate sandstone and conglomerate. Siltstones, mudstones and shales are light grey to olive green with few primary sedimentary structures. Plant fragments and pedogenic structures including abundant rooting and slickensides are abundant (Demchuk and Hills, 1991). Sandstones are very fine- to medium-grained with minor conglomerate as lag deposits overlying erosional contacts with abundant siderite staining. Thin coal and argillaceous units are invariably present. Paleontological studies including

vertebrate paleontology (Fox, 1990), insects (Wighton, 1982), and palynology (Demchuk, 1990) indicate a Paleocene or Upper Paleocene age (Demchuk and Hills, 1991).

Dalehurst Member

The Dalehurst Member is comprised of interbedded sandstone, siltstone, mudstone, shale and coal. The sandstones are predominantly light gray medium- to fine-grained, massive or planar bedded with minor planar cross-bedding and wavy-disturbed bedding. Carbonaceous or coal laminae, plant fragments, and rooting are rare (Demchuk and Hills, 1991). Distinct coal seams ranging from 1.3 m to 6.1 m in thickness are abundant in the Dalehurst Member in comparison to the other two underlying members. The only paleontology investigation of the upper Paskapoo Formation based on palynology (Demchuk, 1990) indicates that the Dalehurst Member covers the uppermost part of the upper Paleocene (Demchuk and Hills, 1991).

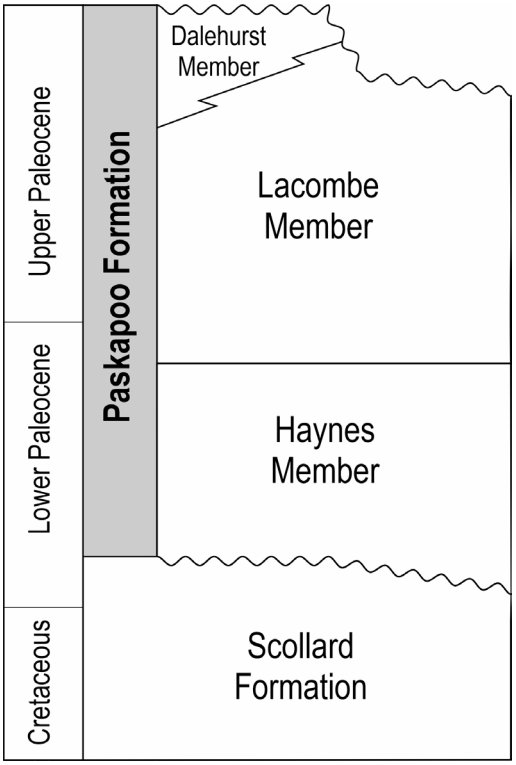

Figure 1. *Stratigraphy of the Paskapoo Formation (modified after Demchuk and Hills, 1991.*

Sampling and Methodology

Samples

Eight shallow monitoring wells (Table 1; Fig. 2) were drilled to collect samples from the Paskapoo Formation in the Fox Creek study area for programmed pyrolysis analysis, organic petrography, and

random vitrinite reflectance (%VRo) to evaluate the thermal maturity of imbedded coal intervals. A total of ninety-seven (97) cutting samples were collected for programmed pyrolysis.

Programmed Pyrolysis

Bulk powdered samples (~70 mg) were analyzed with the HAWK TOC analyzer (Wildcat Technologies) using programmed temperature heating. The pyrolysis stage (under He environment) involved the initial isotemperature of 300°C for 3 min to release free hydrocarbons in the samples (S1, mg HC/g Rock), followed by a ramping temperature of 25°C/min up to 650°C to release, through thermal cracking, hydrocarbons and the oxygen contained in pyrolizable kerogen (S2, mg HC/g rock, and S3, mg CO_2/g rock, respectively).

Samples were then automatically transferred to the oxidation oven and heated from 300°C to 850°C with the heating rate of 20°C per minute to measure the residual inert organic carbon (S4, mg CO and CO_2/g rock and residual carbon (RC) wt.%) and a portion of the mineral carbon (MinC, wt.%). Total organic carbon (TOC, wt. %) is quantified as the sum of the total quantity of OM released during pyrolysis (Pyrolizable Carbon, PC wt. %) and the oxidation step (RC wt. %). Oxygen index (OI) is calculated by normalizing the quantity of the pyrolizable CO_2 (S3) to total organic carbon (S3/TOC ×100) and is proportional to the elemental O/C ratio of the kerogen while the hydrogen index (HI) is the ratio of (S2/TOC × 100) and is proportional to H/C (Behar et al., 2001).

Organic Petrography

To better characterize the type of organic matter and its thermal maturity, eighteen (18) samples throughout the cored intervals were selected based on their TOC and S2 content from different types of lithologies especially coal seams. The selected samples for petrography were examined using a reflected light microscope (Zeiss Axioimager II) equipped with the Diskus-Fossil system following the ASTM (2014) standard. Samples were mounted in cold-setting epoxy polished for organic petrography and reflectance measurements. The standard reference for reflectance measurements was yttrium-aluminum-garnet with a standard reflectance of 0.906% under oil immersion.

Table 1. *Name, length, and location of the shallow monitoring wells drilled in the Paskapoo Formation*

Monitoring well	Depth (m)	Longitude	Latitude	Formation
MW1C	0.0 – 55.0	54.36754737	-117.3811861	Paskapoo
MW3B	0.0 – 49.7	54.37828	-117.117905	Paskapoo
MW3C	0.0 – 49.0	54.37683435	-117.0794847	Paskapoo
MW3D	0.0 – 89.0	54.33204806	-117.0827082	Paskapoo
MW6C	5.0 – 35.0	54.34021596	-117.1484651	Paskapoo
MW6D	0.0 – 51.0	54.34021234	-117.1484852	Paskapoo
MW8C	5.0 – 50.0	54.30045	-117.23566	Paskapoo
MW9A	0.0 – 47.6	54.28559812	-117.2592642	Paskapoo
MW10A	1.0 – 54.0	-	-	Paskapoo

Notes: MW10A was drilled on an active well pad and its location cannot yet be disclosed. Well MW6C is located next to well MW6D and is shallower (35 m). Therefore, no cuttings were sampled from this well.

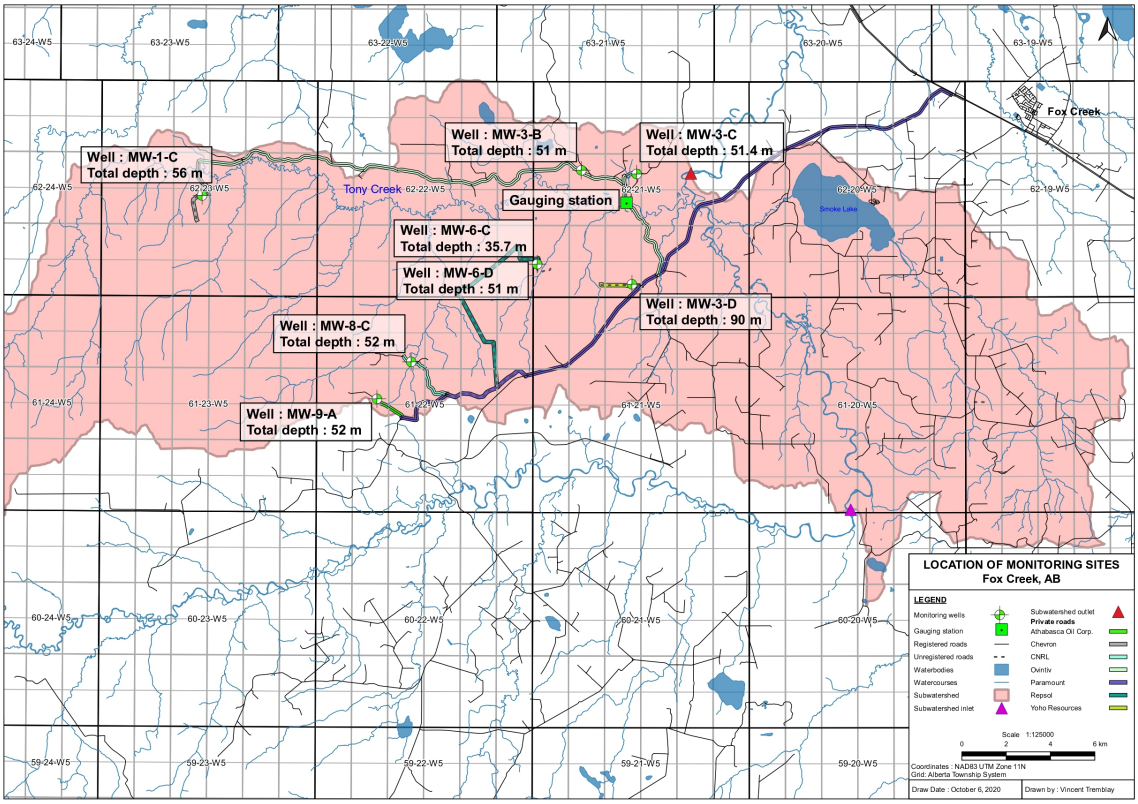

Figure 2. *Location of monitoring wells in the Fox Creek area. The entire (700 km^2) study area of the GSC project is shown in pink,*

Results and Discussion

Lithology of monitoring wells drilled for this study

The detailed lithostratigraphic logs of the shallow monitoring wells drilled for the project (Table 1) are presented in the Appendix 1. Nine monitoring wells were drilled, but no cuttings were collected from MW6C since it is located next to MW6D and shallower (35 m). The top section of the majority of monitoring wells is composed of till sediments and loose sand except for well MW1C, for which the top section is exclusively composed of loose sand (Appendix 1). Medium to fine-grained sandstone alternating with siltstone and shale are the dominant lithologies of the drilled monitoring wells. Three cores (MW1C, MW8C, and MW10A), have coal seams with 20 cm, 80 to 100 cm, and 50 cm thickness, respectively (Appendix 1, Fig. 3). For almost all of the studied samples for organic petrography, vitrinite was the dominant organic maceral.

Programmed Pyrolysis and TOC data

The programmed pyrolysis analysis results of studied samples are presented in Table 2. The S1 (i.e., free hydrocarbon) is extremely low and range from 0.0 to 4.0 (mg HC/g), with a mean and median values

of 0.06 and 0.01 (mg HC/g), respectively (Table 2). The abnormally high S1 value (3.99 mg HC/g) is from a till sample in well MW10A (Table 2). The S2, kerogen and/or liable organic matter, vary over a wide range from 0.02 to 22.9 (mg HC/g) with a mean and median values of 0.77 and 0.09 (mg HC/g), respectively. The majority of samples (63) yield S2 values ≤ 0.2 (mg HC/g), which makes the majority (65%) of Tmax values, temperature at maximum S2 yield and thermal maturity proxy, unreliable (Peters, 1986). Nonetheless, the mean Tmax value for all samples is 434 ± 20°C (n = 97).

Table 2. *Programmed pyrolysis results of samples collected in the upper part of the Paskapoo Formation from the eight studied wells.*

Q#	Sample ID	Pellet#	Depth	S1	S2	PI	S3	Tmax	PC	TOC	RC	HI	OI
			m	mg HC/g	mg HC/g		mg CO_2/g	°C	%	wt.%	%	mg HC/g TOC	mg CO_2/g TOC
Q-033912	MW1C 001		0.0	0.01	0.05	0.20	0.81	442	0.06	0.34	0.28	14	242
Q-033913	MW1C 002		5.0	0.01	0.03	0.29	0.53	449	0.04	0.30	0.26	8	179
Q-033914	MW1C 003		10.0	0.01	0.04	0.25	0.53	463	0.04	0.30	0.26	13	174
Q-033915	MW1C 004		15.0	0.05	0.10	0.32	0.67	438	0.05	0.40	0.35	25	166
Q-033986	MW1C 005		20.2	0.00	0.02	0.25	0.56	452	0.04	0.30	0.26	8	191
Q-033998	MW1C 006		24.0	0.00	0.03	0.19	0.55	443	0.04	0.30	0.25	9	184
Q-033999	MW1C 007		30.0	0.00	0.02	0.22	0.30	444	0.04	0.29	0.25	8	104
Q-034000	MW1C 008		35.0	0.00	0.02	0.23	0.52	429	0.04	0.25	0.21	8	206
Q-033991	MW1C 009		38.0	0.00	0.02	0.24	0.15	433	0.03	0.27	0.24	7	53
Q-033992	MW1C 010		43.0	0.00	0.07	0.10	1.43	448	0.08	0.39	0.31	17	362
Q-034001	MW1C 011	254/21	48.0	0.03	6.32	0.01	3.06	417	0.70	8.12	7.42	77	37
Q-033916	MW1C 012		55.0	0.01	0.07	0.14	0.31	438	0.04	0.35	0.31	18	87
Q-033917	MW3B 001	241/21	0.0	0.06	0.74	0.08	1.71	411	0.14	0.96	0.82	77	178
Q-033918	MW3B 002		5.0	0.02	0.22	0.07	0.57	434	0.07	0.63	0.56	35	91
Q-033919	MW3B 003		10.0	0.02	0.21	0.07	0.58	436	0.06	0.49	0.44	42	117
Q-033993	MW3B 004		12.4	0.01	0.09	0.10	0.34	431	0.04	0.37	0.33	24	91
Q-033920	MW3B 005		19.0	0.01	0.03	0.24	0.30	351	0.04	0.21	0.18	14	140
Q-033921	MW3B 006		24.0	0.01	0.14	0.09	0.45	434	0.05	0.60	0.55	23	75
Q-033922	MW3B 007		29.0	0.01	0.04	0.21	0.21	449	0.03	0.26	0.24	13	81
Q-033923	MW3B 008		34.0	0.01	0.17	0.06	0.59	434	0.06	0.47	0.42	35	124
Q-033994	MW3B 009	251/21	39.0	0.00	0.52	0.02	0.89	442	0.10	1.50	1.40	34	59
Q-033995	MW3B 010		44.0	0.00	0.11	0.07	0.55	462	0.05	0.48	0.43	23	113
Q-033996	MW3B 011	252/21	49.7	0.03	1.08	0.02	2.22	446	0.19	3.77	3.58	28	58
Q-033924	MW3C 001	242/21	0.0	0.18	1.81	0.09	2.90	412	0.28	1.90	1.62	95	152
Q-033925	MW3C 002		4.5	0.02	0.23	0.07	0.58	437	0.05	0.59	0.54	39	97
Q-033926	MW3C 003		9.5	0.01	0.05	0.16	0.24	432	0.03	0.28	0.25	18	85
Q-033927	MW3C 004		14.0	0.01	0.03	0.27	0.17	349	0.02	0.26	0.23	10	67
Q-033928	MW3C 005		19.0	0.00	0.02	0.27	0.29	425	0.03	0.31	0.27	6	93
Q-033929	MW3C 006		24.0	0.01	0.10	0.11	0.32	444	0.04	0.34	0.30	28	96
Q-033930	MW3C 007	243/21	29.0	0.02	0.61	0.02	0.90	437	0.10	1.06	0.96	57	84
Q-033931	MW3C 008		34.0	0.01	0.15	0.08	0.59	442	0.05	0.55	0.50	27	108
Q-033932	MW3C 009	244/21	39.0	0.01	0.58	0.02	0.28	439	0.08	1.07	0.99	54	26
Q-033933	MW3C 010		44.0	0.01	0.04	0.21	0.35	434	0.03	0.34	0.32	11	101
Q-033997	MW3C 011	253/21	49.0	0.01	0.30	0.03	0.54	446	0.07	0.81	0.74	37	66
Q-033934	MW3D 001		0.0	0.02	0.16	0.09	1.10	436	0.06	0.50	0.43	33	222
Q-033935	MW3D 002		4.0	0.01	0.15	0.09	0.61	439	0.05	0.50	0.45	29	122
Q-033936	MW3D 003		9.0	0.02	0.32	0.06	0.48	436	0.06	0.74	0.68	43	65

Q-033937	MW3D 004		14.0	0.02	0.40	0.05	0.60	436	0.07	0.83	0.75	48	72
Q-033938	MW3D 005	245/21	19.0	0.04	0.58	0.06	0.57	431	0.08	1.03	0.95	56	55
Q-033939	MW3D 006		24.0	0.03	0.47	0.07	0.58	431	0.08	0.78	0.70	59	74
Q-033940	MW3D 007		29.1	0.01	0.03	0.27	0.35	437	0.03	0.24	0.21	10	147
Q-033941	MW3D 008		34.0	0.01	0.05	0.19	0.39	439	0.03	0.28	0.24	17	140
Q-033942	MW3D 009		39.5	0.01	0.03	0.27	0.28	424	0.03	0.28	0.25	10	101
Q-033943	MW3D 010		44.0	0.01	0.58	0.02	0.33	438	0.07	1.03	0.95	56	32
Q-033944	MW3D 011		49.0	0.01	0.08	0.12	0.25	437	0.03	0.38	0.34	20	67
Q-033945	MW3D 012		54.0	0.00	0.12	0.07	0.38	438	0.04	0.44	0.40	27	87
Q-033946	MW3D 013		59.0	0.00	0.03	0.24	0.41	420	0.03	0.29	0.26	9	142
Q-033947	MW3D 014		64.0	0.00	0.06	0.14	0.27	432	0.03	0.37	0.35	16	72
Q-033948	MW3D 015		69.0	0.01	0.12	0.09	0.33	436	0.03	0.45	0.42	25	72
Q-033949	MW3D 016		74.0	0.01	0.05	0.16	0.40	435	0.03	0.37	0.33	15	110
Q-033950	MW3D 017		79.0	0.00	0.03	0.25	0.24	422	0.03	0.31	0.28	8	76
Q-033951	MW3D 018		84.0	0.01	0.05	0.18	0.31	440	0.03	0.31	0.29	14	97
Q-033952	MW3D 019		89.0	0.00	0.04	0.20	0.27	420	0.03	0.27	0.24	13	103
Q-033953	MW6C 001		5.0	0.02	0.20	0.07	0.75	443	0.06	0.58	0.52	35	128
Q-033954	MW6C 002	247/21	10.0	0.03	0.50	0.06	0.63	432	0.08	0.89	0.81	56	70
Q-033955	MW6C 003		15.0	0.01	0.12	0.08	0.45	436	0.03	0.53	0.49	22	86
Q-033957	MW6C 005		20.0	0.01	0.16	0.07	0.39	439	0.04	0.53	0.49	30	73
Q-033958	MW6C 006		25.0	0.01	0.10	0.09	0.28	437	0.03	0.37	0.33	27	77
Q-033960	MW6C 008		30.0	0.01	0.04	0.22	0.20	437	0.02	0.24	0.21	16	85
Q-033961	MW6C 009		35.0	0.01	0.06	0.15	0.38	445	0.03	0.32	0.29	17	118
Q-033962	MW6C 010		40.0	0.00	0.04	0.19	0.25	437	0.02	0.26	0.24	13	94
Q-033963	MW6C 011		45.0	0.00	0.05	0.14	0.28	437	0.03	0.29	0.26	18	97
Q-033965	MW6C 013		50.0	0.00	0.04	0.18	0.34	440	0.03	0.31	0.28	14	112
Q-033966	MW8C 014		5.0	0.01	0.04	0.22	0.64	454	0.04	0.38	0.34	10	170
Q-033967	MW8C 015		10.0	0.01	0.18	0.06	0.41	443	0.04	0.56	0.52	33	72
Q-033968	MW8C 017	248/21	15.0	0.04	5.75	0.01	1.13	418	0.56	5.80	5.23	99	19
Q-033970	MW8C 019		20.0	0.01	0.03	0.28	0.19	360	0.03	0.25	0.22	11	73
Q-033971	MW8C 020		23.5	0.00	0.03	0.23	0.28	455	0.03	0.22	0.18	12	127
Q-033972	MW8C 021		28.5	0.00	0.04	0.19	0.25	435	0.04	0.30	0.26	13	82
Q-033973	MW8C 022		33.5	0.01	0.03	0.28	0.42	442	0.04	0.27	0.22	9	156
Q-033974	MW8C 023		38.5	0.01	0.02	0.30	0.34	460	0.03	0.18	0.15	12	185
Q-033975	MW8C 024		43.5	0.01	0.06	0.15	0.27	442	0.04	0.43	0.38	13	64
Q-033976	MW8C 026		50.0	0.00	0.03	0.22	0.26	444	0.04	0.29	0.26	11	89
Q-033977	MW9A 001		0.0	0.04	0.35	0.10	1.54	424	0.11	0.77	0.67	45	198
Q-033978	MW9A 002		5.0	0.00	0.02	0.27	0.56	431	0.04	0.27	0.23	7	204
Q-033979	MW9A 003		10.0	0.00	0.02	0.27	0.45	442	0.04	0.24	0.20	9	185
Q-033980	MW9A 004		15.2	0.00	0.02	0.32	0.39	347	0.04	0.24	0.20	7	164
Q-033981	MW9A 005		20.0	0.00	0.03	0.23	0.34	450	0.03	0.27	0.23	9	126
Q-033987	MW9A 006		25.0	0.00	0.02	0.25	0.52	445	0.04	0.26	0.22	7	199
Q-033982	MW9A 007		31.8	0.00	0.06	0.12	0.48	456	0.05	0.45	0.40	13	105
Q-033983	MW9A 008		35.0	0.00	0.02	0.17	0.29	441	0.04	0.36	0.32	6	80
Q-033988	MW9A 009		40.0	0.00	0.22	0.04	0.44	441	0.05	0.60	0.55	36	72
Q-033984	MW9A 010		45.0	0.00	0.03	0.20	0.36	449	0.04	0.26	0.23	11	136
Q-033985	MW9A 011	249/21	47.6	0.01	1.14	0.01	0.56	441	0.14	2.17	2.04	52	25
Q-033901	MW10A 001	237/21	1.0	3.99	22.92	0.148	12.33	426	2.70	8.56	5.86	267	144
Q-033902	MW10A 002	238/21	4.0	0.23	3.89	0.055	3.18	428	0.47	2.60	2.13	149	122
Q-033903	MW10A 003		9.5	0.02	0.33	0.049	0.49	437	0.06	0.75	0.69	43	64
Q-033904	MW10A 004		14.0	0.02	0.96	0.02	0.73	436	0.12	1.56	1.44	61	47
Q-033905	MW10A 005		19.0	0.01	0.25	0.04	0.33	435	0.06	0.70	0.65	36	47
Q-033906	MW10A 006		24.0	0.02	0.65	0.03	0.54	437	0.09	1.26	1.17	51	43

Q-033907	MW10A 007		29.0	0.03	0.56	0.057	0.69	431	0.09	0.94	0.84	60	73
Q-033908	MW10A 008		34.0	0.03	0.53	0.050	0.70	433	0.09	0.95	0.86	56	73
Q-033909	MW10A 009		39.0	0.01	0.41	0.033	1.86	441	0.12	0.96	0.84	43	193
Q-033910	MW10A 010	239/21	43.0	0.04	9.28	0.00	1.99	424	0.89	8.76	7.87	105	22
Q-033989	MW10A 011		44.0	0.00	0.07	0.11	0.28	445	0.04	0.35	0.32	18	79
Q-033911	MW10A 012	240/21	49.0	0.02	2.34	0.01	0.67	434	0.25	2.77	2.52	84	24
Q-033990	MW10A 013	250/21	54.0	0.03	5.93	0.00	0.68	428	0.56	4.85	4.29	122	14
			mean	0.06	0.77	0.14	0.74	434	0.11	0.95	0.84	33	107
			median	0.01	0.09	0.11	0.45	437	0.04	0.39	0.35	22	93
			stdev	0.40	2.69	0.09	1.32	20	0.30	1.62	1.38	36	57
			max	3.99	22.92	0.32	12.33	463	2.70	8.76	7.87	267	362
			min	0.00	0.02	0.00	0.15	347	0.02	0.18	0.15	6	14
			n	97	97	97	97	97	97	97	97	97	97

The total organic carbon (TOC) content of samples varies over a wide range from 0.2 to 8.8 (wt. %) with a mean and median values of 0.95 and 0.39 (wt. %). The TOC content of the majority of samples (57) is lower than 0.5 (wt. %) and highly variable throughout all studied monitoring well samples (Table 2; Fig. 3). Despite the low mean TOC content of studied samples (0.95 wt. %), a few intervals in wells MW1C, MW3D, MW8C, and MW10A have higher TOC content, up to 8.0% (Table 2, Fig. 3). Most of those intervals consist of thin coal layers. The mean HI and OI values are 33 ± 36 (mg HC/g TOC) and 107 ± 57 (mg CO_2/g TOC), respectively (Table 2).

The programmed pyrolysis pyrograms of samples show that the majority of samples yield extremely low S1 and S2 (Table2, Fig. 4). Due to low S2 yield (≤ 0.2 mg HC/g) and low TOC content (≤ 0.5 wt. %), the majority of HI and OI values are also not be reliable (Peters, 1986). Based on programmed pyrolysis data, there is no significant distinction between different lithologies (Appendix 1), as shown in Figure 5. The pseudo van Krevelen plot (Fig. 5A), as well as the Paskapoo Formation depositional environment (Demchuk and Hills, 1991; Hamblin, 2004) suggest terrestrial organic matter is the dominant organic matter type in the studied samples. In order to investigate the effect of low S2 and TOC content on HI, OI and Tmax values, we removed all samples with S2 < 0.2 mg HC/g and TOC < 0.5 wt. % from the dataset (Fig. 5C-D). The higher Tmax values associated with low S2 were removed, since low S2 values result in flat or bi-modal nature of S2 peaks (Fig. 4), making Tmax evaluation equivocal. Samples with such low S2 values cannot be used as an accurate thermal maturity proxy. Therefore, due to uncertainties in programmed pyrolysis data, organic petrography was needed to confirm the organic matter type and thermal maturity of the studied samples.

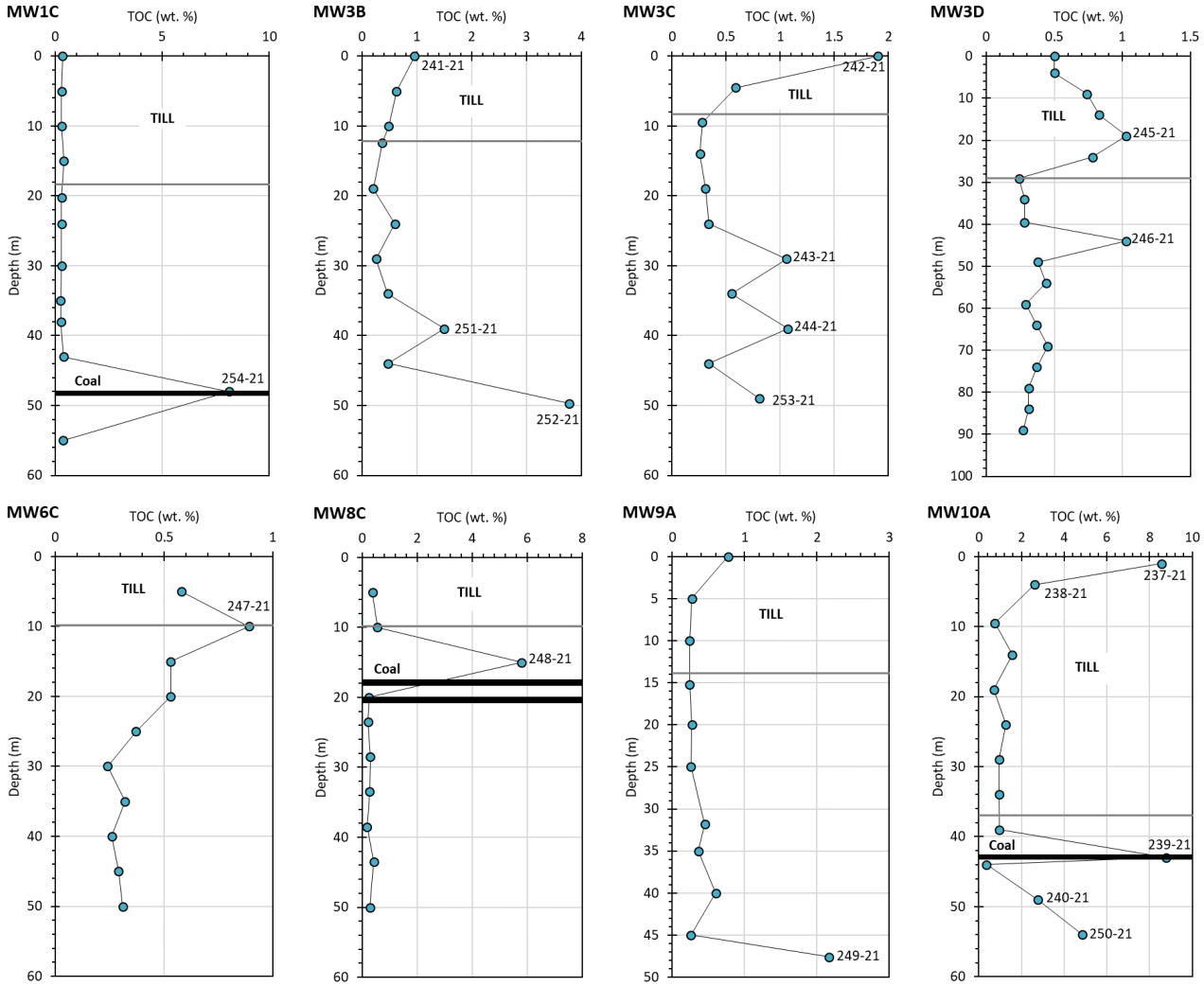

Figure 3. *Total organic carbon (TOC) content variation of the studied samples from each shallow well. The location and depth of organic petrography pellets and coal layers are shown on the profiles.*

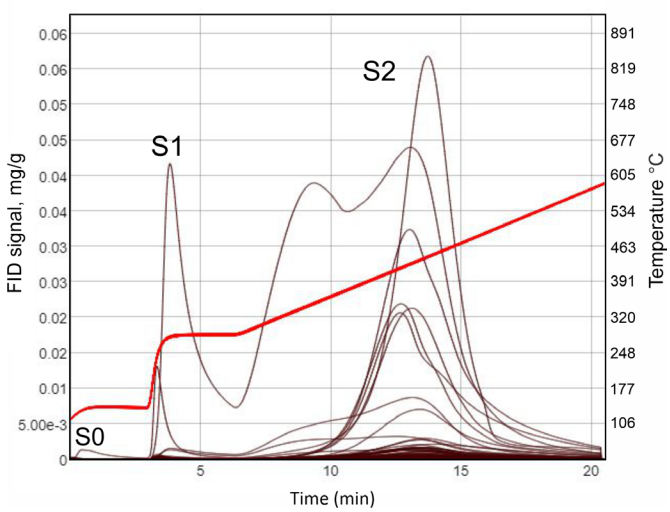

Figure 4. *Programmed pyrolysis pyrograms of the studied samples; the majority of samples yield extremely low S1 and S2 values.*

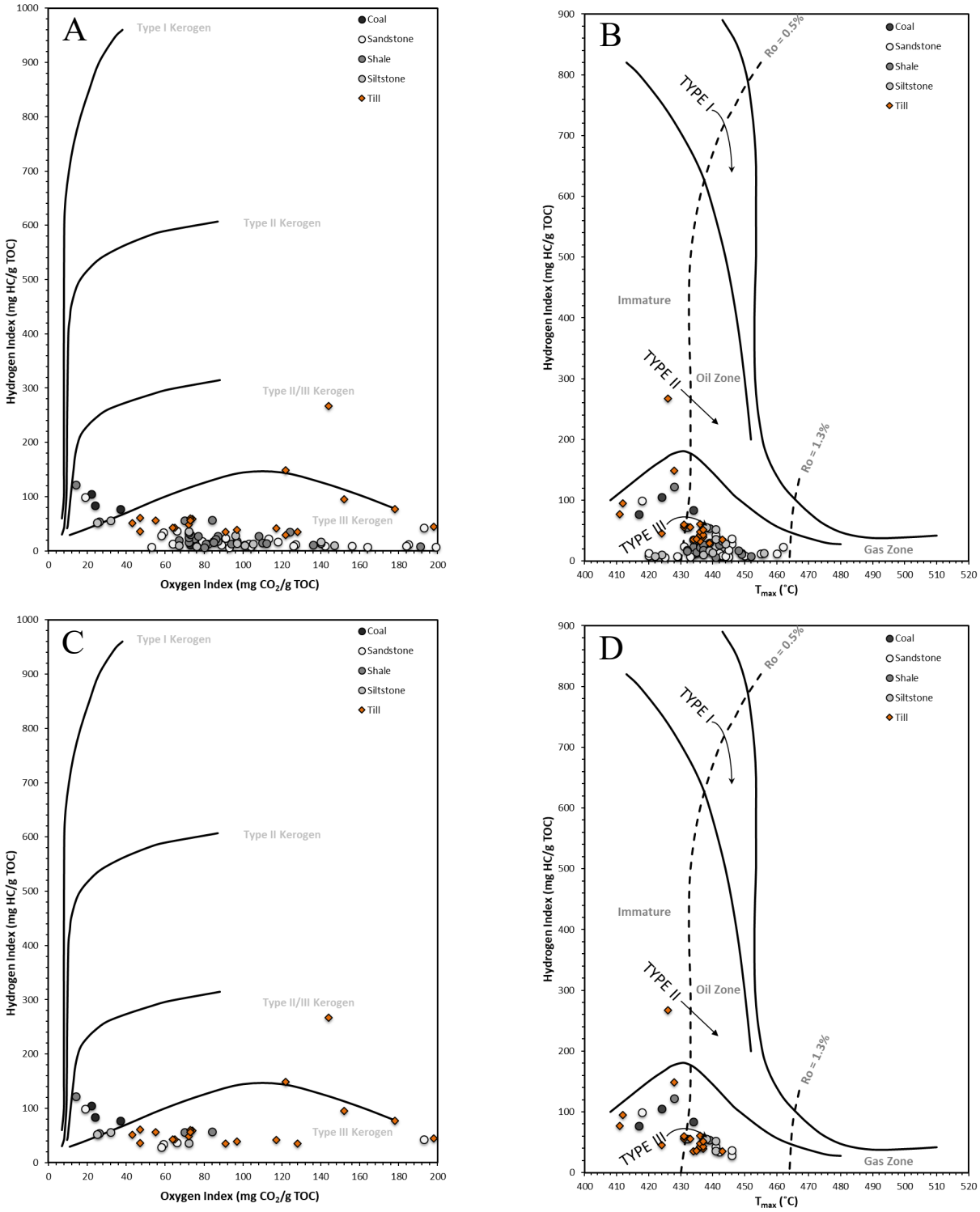

Figure 5. *Programmed pyrolysis plots of the studied samples. (A) pseudo van Krevelen (HI vs. OI), (B) HI vs. Tmax plot, (C) pseudo van Krevelen plot, and (D) HI vs. Tmax after removing samples with S2<0.2 mg HC/g.*

Organic petrography and thermal maturity

In addition to coal seams, organic petrography samples were collected from high TOC intervals (TOC > 0.5%) of the drilled monitoring wells (Fig. 3) in order to identify the dominant organic matter

type and its thermal maturity using random vitrinite reflectance (R_r) measurements. The mean values and summary statistics of measured Rr of the studied samples are reported in Table 3. The organic matter type in all samples except for sample 243/21 is terrestrial organic matter and in order of abundance are (1) vitrinite, (2) inertinite, and (3) liptinite (alginite and sporinite) (Fig. 6). Sample 243/21 is a fine-grained sandstone with minor amount of alginite (Fig. 6M-N).

The maceral composition of all studied samples from till, sandstone, siltstone, shale and coal seams are similar (Fig. 6). However, the mean random vitrinite reflectance (R_r) of the majority of till intervals are lower than deeper intervals in each monitoring well, ranging from 0.25 to 0.29% (Table 3). The mean R_r of one sample from a till interval from monitoring well MW3D (245/21) is, however, markedly higher than the rest of till samples with a mean R_r equal to 0.42 ± 0.03% (n = 45; Table 3). The mean values of R_r of the rock samples (including sandstone, siltstone, shale intervals and coal seams) are higher and vary from 0.39 to 0.49% (Table 3), which is in agreement with the fluorescence color of liptinitic macerals and indicate the immature nature of the studied samples.

Table 3. *Random vitrinite reflectance data of samples collected in the upper part of the Paskapoo Formation from the eight studied wells.*

Pellet#	Q#	Sample Name	Lithology	Depth (m)	mean %R_r	stdev	n
254/21	Q-034001	MW1C 011	COAL	48.0	0.43	0.03	201
241/21	Q-033917	MW3B 001	TILL	0.0	0.26	0.03	39
251/21	Q-033994	MW3B 009	SANDSTONE	39.0	0.44	0.04	100
252/21	Q-033996	MW3B 011	SANDSTONE	49.7	0.40	0.04	77
242/21	Q-033924	MW3C 001	TILL	0.0	0.29	0.07	25
243/21	Q-033930	MW3C 007	SHALE	29.0	–	–	–
244/21	Q-033932	MW3C 009	SHALE	39.0	0.40	0.03	25
253/21	Q-033997	MW3C 011	SANDSTONE	49.0	0.39	0.04	36
245/21	Q-033938	MW3D 005	TILL	19.0	0.42	0.03	45
246/21	Q-033943	MW3D 010	SILTSTONE	44.0	0.40	0.04	66
247/21	Q-033954	MW6C 002	SHALE	10.0	0.49	0.05	9
248/21	Q-033968	MW8C 017	COAL	15.0	0.44	0.05	180
249/21	Q-033985	MW9A 011	SILTSTONE	47.6	0.44	0.05	100
237/21	Q-033901	MW10A 001	TILL	1.0	0.25	0.04	128
238/21	Q-033902	MW10A 002	TILL	4.00	0.27	0.06	66
239/21	Q-033910	MW10A 010	COAL	43.0	0.39	0.03	205
240/21	Q-033911	MW10A 012	COAL	49.0	0.43	0.04	180
250/21	Q-033990	MW10A 013	SHALE	54.0	0.46	0.04	107

The coal particles in till samples are mainly composed of geolvitrinite (Fig. 6B) and corpogelinite (Fig. 6D) which are at the boundary of transition from peatification to vitrinization during biochemical gelification (Fig. 7). Figure 7 illustrates the thermal evolution of terrestrial organic matter and

coalification. The low vitrinite reflectance (0.25 to 0.29%) of till samples and their morphology (Fig. 6B and D) further confirm early stages of coalification (Fig. 7). Coalification refers to progressive changes in composition and structure during diagenetic alteration of deposited terrigenous sedimentary organic matter (Levine, 1993; Table 3). The decomposition and burial of plant debris resulted in occurrence of plant fossils in various stages of diagenetic alteration such as "non-gelified" and "gelified" woods. Biochemical gelification and then diagenetic gelification mainly occurs in low rank coals that resulted in the loss recognizable morphological structures of original plants (Chaffee et al., 1984). Therefore, coal particles in the till samples dominantly originated from a low rank coal or lignite (Fig. 7). In contrast, coal particles from deeper intervals of the studied monitoring wells (Fig. 3), with higher R_r values (0.39 to 0.49%), originated from a relatively higher thermal maturity coal like a sub-bituminous coal, corresponding to a "low rank" coal (Fig. 7).

The measured R_r values are also in agreement with green to yellow fluorescence color of liptinitic macerals (Fig. 6). Exsudatinite (also called exudatinite), a secondary liptinite maceral, as a resinous or asphalt like material are found as fillings or linings of cracks and framboidal pyrite intercrystalline pores of lower intervals of the studied monitoring wells (Fig. 6J-K). Exsudatinite has long been known as a secondary liptinite derived from the transformation of sporinite, alginite, resinite and varieties of vitrinite (Teichmüller, 1974; Teichmüller and Durand, 1983) that forms at stages of heavy oil and bitumen generation in low rank coal (i.e., Ro ~ 0.45%) (Teichmüller, 1974).

The yellow fluorescence color associated with minor alginite macerals observed in fine-grained sandstone interval in well MW3C (pellet 243/21; Fig. 6 M-N) is also in agreement with the overall thermal maturity of other sample underlying tills. Due to presence of exsudatinite in the lower intervals of the studied monitoring wells, additional organic geochemistry analysis from coal-rich samples will be performed to better characterize the nature of pre-oil phases within the Paskapoo Formation to trace any possible contamination in the aquifer.

The R_r values measured for all the studied samples, the fluorescence color of liptinitic macerals (bright green to yellow; Fig. 6) and the presence of exsudatinite all suggest a low rank coal from lignite to sub-bituminous coal (Table 3; Fig. 7). Although the range of programmed pyrolysis Tmax (347 to 463°C) overestimates the thermal maturity of the samples in many cases (Table 2; Fig. 5 B), the Tmax values of samples with S2 > 0.2 mg HC/g suggest early to peak oil window thermal maturity. However, based on random vitrinite reflectance and fluorescence microscopy, the organic matter in the studied intervals is considered immature and composed of lignite and sub-bituminous coal. The low S2 peaks of the studied cutting samples are likely the main reason for the inaccuracy of the Tmax values (e.g., Peters, 1986; Yang and Horsfield, 2020). This result further emphasizes the importance and relevance

of organic petrography, reflectance measurement, and fluorescence microscopy in accurately estimating the thermal maturity of sedimentary rocks.

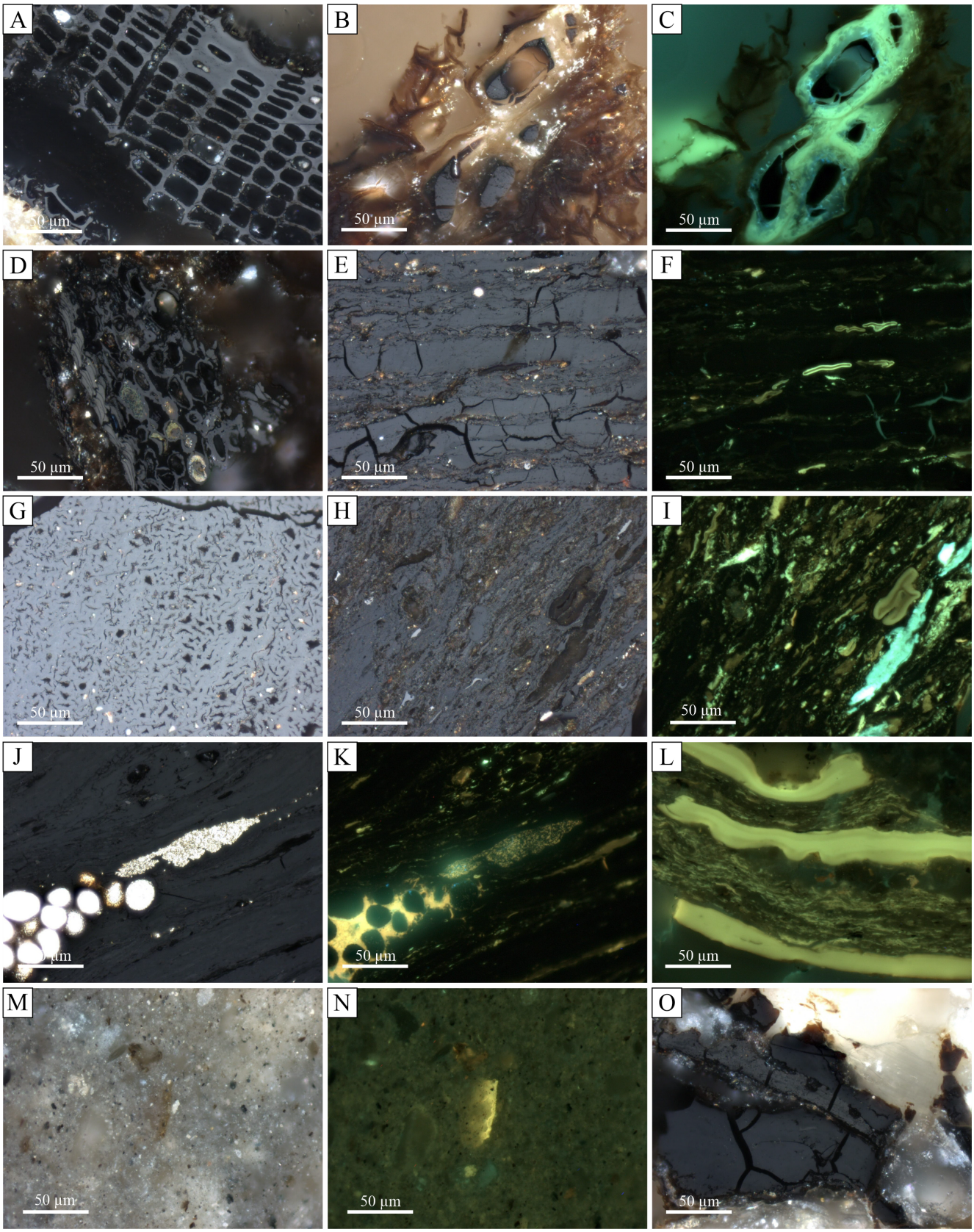

Figure 6. *Photomicrographs of studied samples with incident white and ultra violet (UV) light under oil immersion with ×50 objective. (A) Large inertinite particle from till samples. (B) Gelified plant particles turned to gelovitrinite: this vitrinite sample has the lowest R_r (~0.25%); the gelified particles are more abundant in till samples. (C) Same view as image B but under UV light: unaltered plant particles exhibit blue to green fluorescence indicative of the low maturity of the sample. (D) Low reflectance corpogelinite (right of the image)(~0.25%) and suberinite (left of the image)in the till samples. (E-F) Pair view under white (E) and UV light (F) shows a big vitrinite particle with desiccation cracks. Green fluorescing sporinite are scattered in vitrinite, visible under UV light. (G) Big piece of inertinite (fusinite) in Paskapoo Formation. (H-I) Pair view under white (H) and UV light (I) shows a big piece of vitrinite with scattered inertinite (H), abundant green-yellow fluorescing sporinite and blue fluorescing alginite visible under UV light (I). (J-K) Pair view under white (J) and UV light (K) shows a big piece of vitrinite with abundant fine-crystalline pyrite and framboidal pyrite (J), yellow-orange fluorescing exsudatinite accumulated within pyrite intercrystalline pores (K). (L) Big pieces of green fluorescing megasporinite and alginite. (M-N) Pair view under white (M) and UV light (N) shows a fine-grained siltstone with yellow fluorescing alginite. (O) Big pieces of vitrinite within a coarse-grained fabric.*

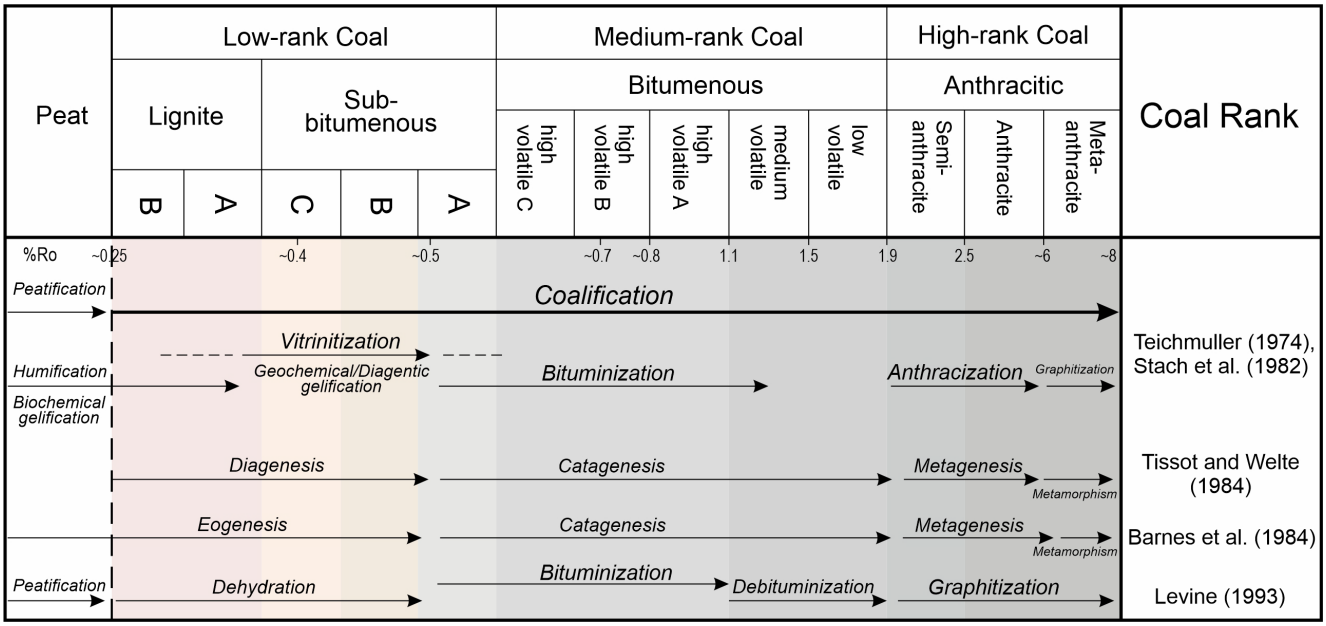

Figure 7. *Stages of coalification process and coal ranks at different stages of thermal evolution of terrestrial organic matter (modified after [Kentucky Geological Survey Coal Classification]).*

Potential contamination of shallow groundwater from coal seams

Hydrocarbon origin

It is commonly assumed that low rank coals do not generate hydrocarbons during maturation. However, low rank coals can generate biogenic gas (Rice and Claypool, 1981) and some (such as Canadian Arctic immature coals) were found to generate oily exudates (e.g., Snowdon and Powell, 1982). The R_r values obtained from all samples (Table 3) indicate that terrigenous organic matter is still

immature and did not generate liquid or gas hydrocarbon except exsudatinite. Exsudatinite generally derives from the transformation of sporinite, alginite, resinite and varieties of vitrinite, which is a resinous or asphaltic like material (Teichmüller, 1974) commonly observed in coals having Rr < 0.5%, below the classic thermogenic "oil window" (Levine, 1993). Therefore, considering the very thin thickness and scattered distribution of coal seams in the studied samples, it is unlikely the exsudatinite is a major source of hydrocarbons to the shallow aquifer in the study area. However, additional stratigraphic studies, molecular geochemistry, and biomarker analysis could help estimate the potential of possible organic compound contribution to the aquifer in the study area.

Contribution to the generation of biogenic methane

Decomposition of organic matter at low temperatures by anaerobic microorganisms generates biogenic methane with distinctive significantly depleted $\delta^{13}C$ (i.e., ≤ -55‰) due to kinetic isotope fractionation by methanogens (Rice and Claypool, 1981). Biological activity and chemical rearrangement during diagenesis (Fig. 7) of immature organic matter is responsible for kerogen formation, which is the source of most hydrocarbons. Biogenic methane is the only hydrocarbon compound that could be generated at this stage in significant volumes (Rice and Claypool, 1981).

The main potential sources of hydrocarbon "contamination" in shallow groundwater in proliferous sedimentary basins such as WCSB that contains numerous organic-rich sedimentary rocks, are; (i) natural in-situ production of biogenic methane, (ii) leakage of biogenic or thermogenic methane into shallow aquifers from faulty oil and gas wells, and (iii) migration of thermogenic methane from deep reservoirs through fault systems or due to conventional and unconventional hydrocarbon resource exploitation (Osborn et al., 2011; Atkins et al., 2015; Humez et al., 2016). In a regional study on methane formation and migration in Alberta shallow aquifers that included the Paskapoo Formation, evidence of biogenic methane, sometimes also combined with thermogenic methane, is provided (Humez et al., 2016).

Conclusion

Ninety-seven (97) cutting samples from the Paskapoo Formation were obtained from eight shallow monitoring wells (50-90 m) in the Fox Creek area in west-central Alberta to measure TOC content, organic matter composition and thermal maturity of coal seams using programmed pyrolysis analysis in order to investigate any potential internal hydrocarbon source within the Paskapoo Formation, the main shallow aquifer in Alberta. The TOC content ranges from 0.2 to 8.8 wt. %, with a mean value of 0.95 ± 1.6 wt. % (n =97). The Tmax value of the studied samples range from 347 to 463 °C, with a mean value of 434 ± 20 °C that suggest a range of thermal maturity from immature to peak oil window.

The random reflectance (R_r) measurements and fluorescence microscopy observations were performed on eighteen (18) samples with TOC content greater than ~1 wt. % to estimate the thermal maturity of the upper part of the Paskapoo Formation. The mean R_r value of the overlying till deposits is equal to 0.27%, while the mean R_r value of the underlying sandstone, siltstone, shale and coal seams is equal to 0.42%, indicating a low rank coal ranging from lignite to sub-bituminous coal. Although the organic matter in the studied intervals is immature, exsudatinite, as secondary liptinite maceral, was observed in samples from the lower parts of the studied monitoring wells.

Exsudatinite, a type of oily residue has been recognized in some coal samples. Considering the thin thickness and scattered distribution of coal seams in the studied samples, it is unlikely that the exsudatinite will be a major source of hydrocarbon contamination in shallow groundwater in the study area. Due to the presence of dispersed organic matter and coal seams in the study area, biogenic methane formation is likely, therefore, it is important that the potential of biogenic methane formation in the Paskapoo shallow aquifers be investigated.

Acknowledgements

The authors would like thank K. Boyce, P. Webster, and C. Gallotta of Geological Survey of Canada, Calgary for sample handling and preparation and R. Vandenberg for programmed pyrolysis analysis. Helpful comments provided by Drs. D. Lavoie and C. Jiang on the initial draft of the report and comments on organic petrography by J. Reyes is appreciated. The monitoring stratigraphy logs were created by V. Tremblay, his assistance is appreciated. This work is supported by Natural Resources Canada (NRCan) Environmental Geoscience program.

References

Allan, J.A. and Sanderson, J.O.G. 1945. Geology of the Red Deer and Rosebud map-sheets. Alberta Research Council, Report 13, 109p.

ASTM. (2014). Standard Test Method for Microscopical Determination of the Reflectance of Vitrinite Dispersed in Sedimentary Rocks D7708-14. In *ASTM*. ASTM. https://doi.org/10.1520/D7708-14

Atkins, M. L., Santos, I. R., & Maher, D. T. (2015). Groundwater methane in a potential coal seam gas extraction region. *Journal of Hydrology: Regional Studies*, *4*, 452–471. https://doi.org/10.1016/J.EJRH.2015.06.022

Barnes, M. A., Barnes, W. C. & Bustin, R. M. (1984). Diagenesis 8. Chemistry and Evolution of Organic Matter. *Geoscience Canada*, *11*(3), 103–114.

Behar, F., Beaumont, V., De, H. L., & Penteado, B. (2001). Rock-Eval 6 Technology: Performances and Developments. *Oil & Gas Science and Technology-Rev. IFP*, *56*(2), 111–134.

Chaffee, A. L., Johns, R. B., Baerken, M. J., de Leeuw, J. W., Schenck, P. A., & Boon, J. J. (1984). Chemical effects in gelification processes and lithotype formation in Victorian brown coal. *Organic Geochemistry*, *6*(C), 409–416. https://doi.org/10.1016/0146-6380(84)90063-9

Digiulio, D. C., & Jackson, R. B. (2016). Impact to Underground Sources of Drinking Water and Domestic Wells from Production Well Stimulation and Completion Practices in the Pavillion,

Wyoming, Field. *Environmental Science and Technology*, *50*(8), 4524–4536. https://doi.org/10.1021/acs.est.5b04970

Demchuk, T. D. (1990). Palynostratigraphic zonation of Paleocene strata in the central and south-central Alberta Plains. *Canadian Journal of Earth Sciences*, *27*(10), 1263–1269. https://doi.org/10.1139/e90-136

Demchuk, T. D., & Hills, L. v. (1991). A re-examination of the Paskapoo Formation in the central Alberta Plains: the designation of three new members. *Bulletin of Canadian Petroleum Geology*, *39*(3), 270–282. https://doi.org/10.35767/gscpgbull.39.3.270

Flewelling, S. A., & Sharma, M. (2014). Constraints on upward migration of hydraulic fracturing fluid and brine. *Groundwater*, *52*(1), 9–19. https://doi.org/10.1111/gwat.12095

Fox, R.C. 1990. The succession of Paleocene mammals in western Canada. In: Dawn of the Age of Mammals in the Northern Part of the Rocky Mountain Interior, T. Bown and K. Rose (eds.). Geological Society of America, Special Paper 243, p. 51-70.

Grasby, S. E., Chen, Z., Hamblin, A. P., Wozniak, P. R. J., & Sweet, A. R. (2008). Regional characterization of the Paskapoo bedrock aquifer system, southern AlbertaGeological Survey of Canada Contribution 2008-0479. *Canadian Journal of Earth Sciences*, *45*(12), 1501–1516. https://doi.org/10.1139/E08-069

Hamblin, A.P. (2004) Paskapoo-Porcupine Hills formations in western Alberta: synthesis of regional geology and resource potential. Geological Survey of Canada, Open File 4679, 2004, 30 pages, https://doi.org/10.4095/215631

Humez, P., Mayer, B., Nightingale, M., Becker, V., Kingston, A., Taylor, S., Bayegnak, G., Millot, R., & Kloppmann, W. (2016). Redox controls on methane formation, migration and fate in shallow aquifers. *Hydrology and Earth System Sciences*, *20*(7), 2759–2777. https://doi.org/10.5194/hess-20-2759-2016

Lavoie, D., Ardakani, O.H., & Rivard, C. (2021) Synthesis of organic matter composition and maturation and gas data from selected deep source rock units for some wells in the Fox Creek area; Geological Survey of Canada, Open File 8788, 95 p. https://doi.org/10.4095/328238

Lerbekmo, J. F., & Sweet, A. R. (2007). Magnetobiostratigraphy of the continental Paleocene upper Coalspur and Paskapoo formations near Hinton, Alberta. *Bulletin of Canadian Petroleum Geology*, *56*(2), 118–146. https://doi.org/10.2113/gscpgbull.56.2.118

Levine, J. R. (1993). Coalification: The Evolution of Coal as Source Rock and Reservoir Rock for Oil and Gas. In *Hydrocarbons from Coal*. American Association of Petroleum Geologists. https://doi.org/10.1306/St38577C3

Osborn, S. G., Vengosh, A., Warner, N. R., & Jackson, R. B. (2011). Methane contamination of drinking water accompanying gas-well drilling and hydraulic fracturing. *Proceedings of the National Academy of Sciences*, *108*(20), 8172–8176. https://doi.org/10.1073/pnas.1100682108

Peters, K. E. (1986). Guidelines for Evaluating Petroleum Source Rock Using Programmed Pyrolysis'. *AAPG Bulletin*, *70*(3), 318–329.

Rice, D. D., & Claypool, G. E. (1981). Generation, Accumulation, and Resource Potential of Biogenic Gas. *AAPG Bulletin*, *65*. https://doi.org/10.1306/2F919765-16CE-11D7-8645000102C1865D

Ryan, M. C., Alessi, D., Mahani, A. B., Cahill, A., Cherry, J., Eaton, D., Evans, R., Farah, N., Fernandes, A., Forde, O., Humez, P., Kletke, S., Ladd, B., Lemieux, J., Mayer, B., Mayer, K. U., Molson, J., Muehlenbachs, L., Nowamooz, A., & Parker, B. (2015). Subsurface Impacts of Hydraulic Fracturing : Contamination, Seismic Sensitivity, and Groundwater Use and Demand Management. In *Canadian Water Network*.

Smerdon, B.D., Klassen, J. and Gardner, W.P. (2019): Hydrogeological characterization of the Upper Cretaceous–Quaternary units in the Fox Creek area, west-central Alberta; Alberta Energy Regulator/Alberta Geological Survey, AER/AGS Report 98, 35 p.

Snowdon, L. R., & Powell, T. G. (1982). Immature Oil and Condensate--Modification of Hydrocarbon Generation Model for Terrestrial Organic Matter. *AAPG Bulletin*, *66*. https://doi.org/10.1306/03B5A313-16D1-11D7-8645000102C1865D

Stach, E., Mackowsky, M., Teichmüller, M., Taylor, G. H., Chandra, D., & Teichmüller, R. (1982) *Stach's Textbook of Coal Petrology*. 535 p.

Teichmüller, M. (1974). Generation of petroleum-like substances in coal seams as seen under the microscope. *Advances in organic geochemistry*, 321-349.

Teichmüller, M., & Durand, B. (1983). Fluorescence microscopical rank studies on liptinites and vitrinites in peat and coals, and comparison with results of the rock-eval pyrolysis. *International Journal of Coal Geology*, *2*(3), 197–230. https://doi.org/10.1016/0166-5162(83)90001-0

Tissot, B. P., & Welte, D. H. (1984). *Petroleum Formation and Occurrence*. Springer Berlin Heidelberg. https://doi.org/10.1007/978-3-642-87813-8

Vidic, R. D., Brantley, S. L., Vandenbossche, J. M., Yoxtheimer, D., & Abad, J. D. (2013). Impact of shale gas development on regional water quality. In *Science* (Vol. 340, Issue 6134). American Association for the Advancement of Science. https://doi.org/10.1126/science.1235009

Wighton, D. C. (1982) Middle Paleocene insect fossils from south-central Alberta. In: Third North American Paleontological Convention Proceedings, Volume 2, B. Mamet and M.J. Copeland (eds.). Departement de Geologie, Universit6 de Montreal, p. 577-578.

Yang, S., & Horsfield, B. (2020). Critical review of the uncertainty of Tmax in revealing the thermal maturity of organic matter in sedimentary rocks. *International Journal of Coal Geology*, *225*, 103500. https://doi.org/10.1016/j.coal.2020.103500